The Effect of Distortion on the Buckling Strength of Stiffened Panels

Pretheesh Paul C[1*], Purnendu K. Das[1], Anthony Crow[2], Stuart Hunt[2]

[1]*Department of Naval Architecture and Marine Engineering*
Universities of Glasgow and Strathclyde, Glasgow, United Kingdom
[2]*BVT Surface Fleet Ltd.*

*Corresponding author
E-mail address: pretheesh.chaithanya@strath.ac.uk

Abstract

This paper predicts the behaviour of stiffened plates with different distortion levels in order to address a rational structural design procedure as pre-existing and fabrication related (like weld-induced) initial geometrical distortion is of great importance in structural design point of view. The considered range of scantlings, the distortion types and levels were chosen, based on panels used at BVT Surface Fleet Ltd., where the type 45 destroyer were under construction. An analytical relation is presented based on Perry's column approach to establish the variation of buckling strength against the geometrical distortion. A parametric form of non linear finite element analysis using ABAQUS has been carried out under axial loading condition to predict the behaviour and the buckling strength. The effect of residual stress is not considered in this study. A new strength parameter is proposed to represent buckling strength which takes into account the inelastic post-buckling behaviour of the structure. The results from FE analysis are plotted in non-dimensional terms and arrived at some important conclusions.

Key words: stiffened panels; initial distortion; buckling strength; abaqus

Nomenclature

a	length of the plate (in x-direction)
b	width of the plate (in y-direction)
$b_e = b\left(\frac{2}{\beta} - \frac{1}{\beta^2}\right)$	Effective width of plate when, $\beta \geq 1$
h	Height of stiffener web (in z-direction)
m	Number of half waves in the longitudinal (x) direction
n	Number of half waves in the transverse (y) direction
r	Radius of gyration
t	Plate thickness
v_s	Stiffener warping (Maximum)
w_p	Plate distortion (Maximum)
w_s	Stiffener Bowing (Maximum)
y_e	Distance to the extreme fibre at the compression side
E	Young's modulus

L_e	Equivalent length of the column
OBP	Offset Bulk Plate
S	New Strength parameter
$\beta = \frac{b}{t}\sqrt{\frac{\sigma_y}{E}}$	Plate slenderness parameter
δ	Mid span deflection of the beam
δ_0	Initial deflection of the beam
ε_y	Ultimate strain
ϕ_p	Non dimensional plate distortion
ϕ_b	Non dimensional stiffener bowing
ϕ_w	Non dimensional stiffener warping
$\lambda = \frac{a}{\pi r}\sqrt{\frac{\sigma_y}{E}}$	Column slenderness parameter
σ_c	Critical buckling stress
σ_u, σ_{u1}	Ultimate stress
σ_{u2}	Ultimate stress at double the ultimate strain
σ_y	Yield stress

1. Introduction

The influence of weld-induced initial distortions and other deformations in structural design are of great importance as it is essential for the prediction of the behaviour of stiffened and unstiffened plate elements under different loading conditions. Most of the existing studies consider typical initial imperfections as a combination of geometrical distortion and the residual stress. This paper specifically considers distortion as a parameter in assessing buckling strength.

The closed form solutions (Troitsky 1976) for plated structures are insufficient to judge the imperfection sensitivity on the buckling strength precisely and explicitly. When the structure is stocky, the inelastic buckling strength cannot be solved satisfactorily with the analytical formulas as these formulas are based on assumptions valid in a narrow elastic range. An empirical relation by (Paik and Thayamballi 2004) also gives results for the stiffened plates. The effect of initial distortion and residual stress is incorporated implicitly. A simple design equation is proposed by (Ozguc, Das and Barltrop 2007) for the imperfect plates but it does not represent the distortion sensitivity. Since the performance of the stiffened plates are too complex and non-linear beyond the elastic range, it is quite difficult to define a closed form analytical equation for the strength of such structures incorporating every minute aspects of the overall phenomenon.

The combinations of scantlings chosen for this study are typical of upper decks of ships and are lighter compared to the bottom structure. They are hence vulnerable to buckling failure during sagging condition as an extreme axial compression case. This study is restricted to find results for a limited range of scantlings which are commonly used in 'Type 45 Destroyer' produced by BVT Surface Fleet Ltd., and is represented with a non-dimensional design curve form.

Since the fabrication processes like welding, bolting etc. involves forced levelling and constraining of the plate edges during and after the processes, the actual level of the initial deformation, either built in or weld induced, can be observed only at the non-welded sides of the plate. The observable deformation on plates welded along four sides is found to be roughly 10% to 20% of the deformation at non-welded plate edges. The deformation values used in this study correspond to the lowest and the highest deformations observed from the production floor.

The forms of initial distortion in actual structure are highly complex. To represent them accurately, a combination and superimposition of various modes and forms of distortions at random amplitudes would be required. This study assesses two specific forms: A sinusoidal form and a 'cusp' form. The frequency of 'cusp' shaped distortion as shown in Figure 9 is found especially at plate butts. The magnitude of imperfections measurements from the BVT construction site are found to be in close agreement with the parametric relations proposed by Dow and Smith (Dow and Smith 1984) as the typical initial plate imperfections – low, average and severe.

A rigorous non-linear finite element analysis of stiffened panels, in ABAQUS, has been undertaken in order to find out the influence of the initial distortions on their buckling strength reduction. There are other factors that may affect the buckling strength of the plated structures like residual stresses, the crystallographic material property changes etc. This study considers only the effect of geometrical distortion on the buckling strength. It will thus be possible to separate the contribution of each of the factors to the change of strength.

2. Scantlings and Distortions

The scantlings commonly used on the Type 45 Destroyer, chosen for the study, are shown in Table 1. This particular vessel, 152.4m long, will be the most advanced anti-aircraft warship in the World, when completed. The total plate tonnage used in the vessel is 3950 tonnes, of that the thin plate proportion is 40% (19% is 4 and 5mm thick: 21% is 6 and 8mm thick). The steel grade is Lloyds' DH 36, which has allowed a weight reduction to be obtained against the original design that was based on Lloyds' grade D steel. From the design viewpoint, the use of DH 36 is a solution to a number of constraints, but has resulted in a thin plate welded structure, which by its nature has introduced a potentially significant distortion problem.

Table 1. Panel scantlings used in the study

Stiffener (OBP)	Plate thk, (mm)	β	a/b=3		a/b=1	
			λ	(σ_c/σ_y)	λ	(σ_c/σ_y)
120x6	5	5.85	0.62	0.90	0.21	0.99
120x6	8	3.65	0.72	0.87	0.24	0.99
120x6	12	2.44	0.90	0.80	0.30	0.98
160x8	5	5.85	0.45	0.95	0.15	0.99
160x8	8	3.65	0.49	0.94	0.16	0.99
160x8	12	2.44	0.57	0.92	0.19	0.99
200x8.5	5	5.85	0.36	0.97	0.12	1.00
200x8.5	8	3.65	0.37	0.97	0.12	1.00
200x8.5	12	2.44	0.41	0.96	0.14	1.00

Stiffener spacing is 700mm for all the cases

According to column approach, which assumes axial symmetry, the critical buckling stresses of these scantlings as per Johnson-Ostenfeld formula (Paik and Thayamballi 2004) are shown in Figure 1. Table 1 illustrate the column slenderness, λ and corresponding critical buckling stress values, σ_c/σ_y calculated based on equivalent width of the plate (Faulkner et al. 1988). All of the selected scantlings appear to fall in the stocky range.

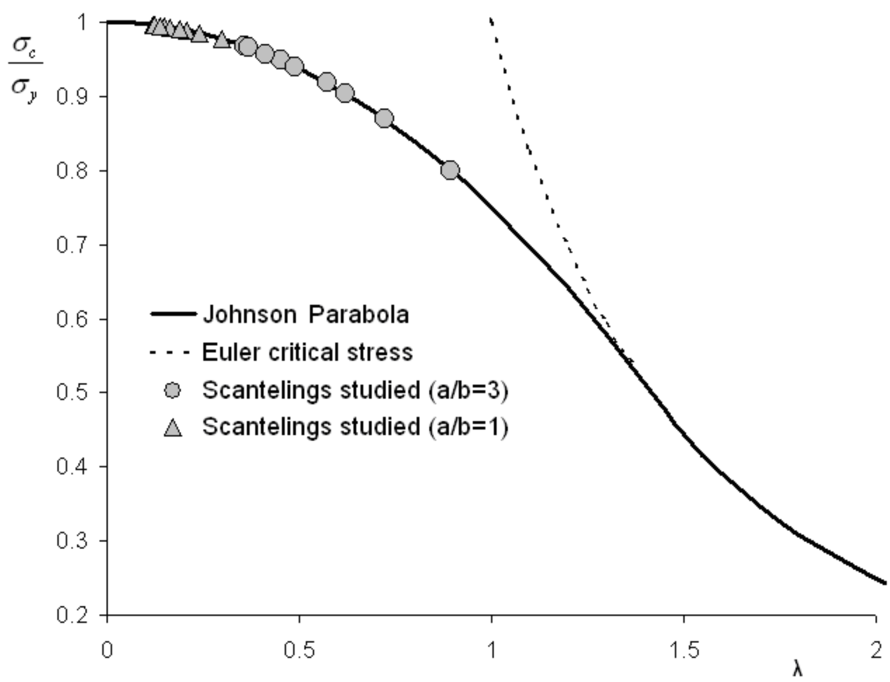

Figure 1. Column Buckling Analysis using Johnson Parabola.

In most of the studies, the initial distortion for the stiffened panel is incorporated with a correction factor while calculating the ultimate strength. This study takes the initial distortion and its magnitude as the primary parameter. The initial distortion can be considered as a combination of distortions observed separately in plates and stiffeners. This study takes into account Plate distortion (wp), Stiffener Bowing (ws) and Stiffener warping (vs). The positive directions of the above mentioned distortions used in this study are as shown in Figure 2.

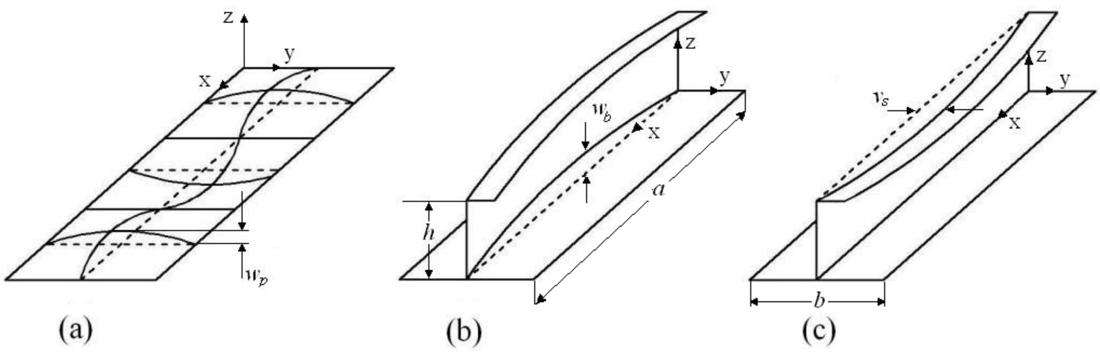

Figure 2. (a) Plate distortion (b) Stiffener bowing (c) Stiffener warping

The geometry of sinusoidal distortions shown in Figure 8 are defined as per the functions given in equations (2.1)-(2.3)

$$w_p(x, y) = w_p \sin\left(\frac{n\pi x}{a}\right)\sin\left(\frac{n\pi y}{b}\right) \qquad (2.1)$$

$$w_s(x, y) = w_b \sin\left(\frac{\pi x}{a}\right) \qquad (2.2)$$

$$v_s(x, z) = v_s \sin\left(\frac{\pi x}{a}\right)\sin\left(\frac{0.5\pi z}{h}\right) \qquad (2.3)$$

The cusp shaped distortions shown in Figure 9 are defined as per the functions given in equations (2.4)-(2.6). The coefficients of equation (2.4) and equation (2.6) are chosen through curve fitting based on typical measurements from BVT construction site.

$$w_p(x, y) = 1.59 w_p \left[0.5^{2/3} - \left(\frac{x}{a} - 0.5\right)^{2/3}\right]\sin\left(\frac{n\pi y}{b}\right) \qquad (2.4)$$

$$w_s(x, y) = w_b \sin\left(\frac{\pi x}{a}\right) \qquad (2.5)$$

$$v_s(x, z) = 1.59 v_s \left[0.5^{2/3} - \left(\frac{x}{a} - 0.5\right)^{2/3}\right]\sin\left(\frac{0.5\pi z}{h}\right) \qquad (2.6)$$

Three levels of 'Initial imperfections' defined by (Smith et al. 1988) based on their experience of representative structures is the widely accepted parametric representation of initial distortion for most of the relevant studies. In this study, theses 'Initial imperfections' are taken only to provide a range for the plate distortion. The plate distortion measurements carried out in the BVT construction site is in close agreement with the above criteria. Table 2 shows the numerical values of the plate distortion

Table 2. Numerical values of the plate distortion

Plate thk.	Amplitude	Plate distortion (mm)
5mm	Light	4.27
	Medium	17.10
	Severe	51.29
8mm	Light	2.67
	Medium	10.68
	Severe	32.05
12mm	Light	1.78
	Medium	7.12
	Severe	21.37

Table 3 shows the numerical values of the stiffener bowing and warping obtained from a series of measurements carried out at the BVT construction site.

Table 3. Numerical values of the stiffener bowing and warping

OBP	Amplitude	a/b=3		a/b=1	
		Bowing (w_s)	Warping (v_s)	Bowing (w_s)	Warping (v_s)
120X6	Light	0	0	0	0
	Medium	5.13	4.53	0	0.5
	Severe	10.26	9.05	0.57	1.01
160X8	Light	0	0	0	0
	Medium	3.85	3.5	0.43	0.39
	Severe	7.69	6.99	0.85	0.78
200X8.5	Light	0	0	0	0
	Medium	3.08	2.75	0.34	0.31
	Severe	6.15	5.5	0.68	0.61

The non dimensional distortion parameters for plate distortion, stiffener bowing and stiffener warping are represented as per equations (2.7)-(2.9) respectively. These parameters are used latter on in the design curves for different types and levels of distortion.

$$\phi_p = \frac{w_p}{t} \qquad (2.7)$$

$$\phi_b = \frac{w_s}{t} \qquad (2.8)$$

$$\phi_w = \frac{v_s}{t} \qquad (2.9)$$

3. Distortion sensitivity as per Perry's approach

An analytical relation based on the column model to represent the effect of initial distortion on the buckling strength of a column structure undergoing axial compression is discussed here. When we use both the Euler's critical stress and the Perry's magnification factor in the first yield criteria, we will be able to arrive at a relation for the ultimate strength of the Euler column based on the initial distortion as a basic variable. It yields a quadratic equation for the Ultimate strength as given below.

$$\left(\frac{\sigma_u}{\sigma_y}\right)^2 - \left(\frac{\sigma_u}{\sigma_y}\right)\left[1+\frac{1}{\lambda^2}+\frac{y_e\delta_0}{\lambda^2 r^2}\right]+\frac{1}{\lambda^2}=0 \tag{3.1}$$

The solution for the above quadratic equation will give the value of ultimate strength of the column as,

$$\left(\frac{\sigma_u}{\sigma_y}\right)=\left[\frac{1}{2}\left(1+\frac{1}{\lambda^2}+\frac{y_e\delta_0}{\lambda^2 r^2}\right)\right]-\frac{1}{2}\sqrt{\left(1+\frac{1}{\lambda^2}+\frac{y_e\delta_0}{\lambda^2 r^2}\right)^2-\frac{4}{\lambda^2}} \tag{3.2}$$

To extend the column approach to stiffened plates, a plate stiffener combination with the effective width of plating is (Faulkner et al. 1988) as shown in Figure 3 is considered as an equivalent column model.

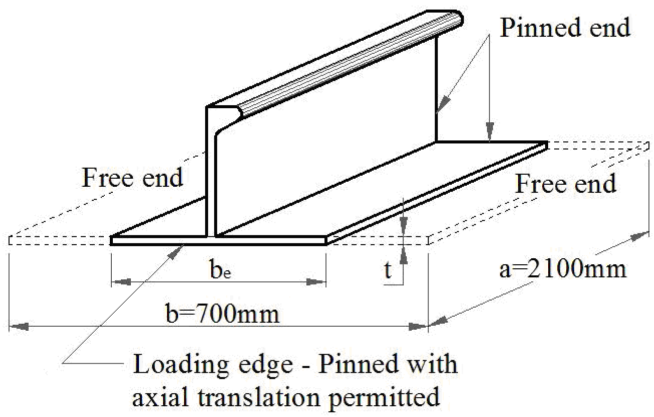

Figure 3. Equivalent column model of the stiffened plate

Figure 4 shows the variation of buckling strength against the distortion according to the above formula, equation (3.2). Three representative equivalent column models similar to scantlings used for plate analysis further in this paper are being plotted. The curves are responsive to both the initial distortion and to the slenderness of the structure. The analysis according to this formula only describes an elastic limit approach to the buckling of the column, which is only valid where inelastic behaviour is unimportant. However, the area of interest in this study is mainly in the inelastic region. The distortion range shown in Figure 4 is not confined to the elastic range in order to represent distortion used further in this paper.

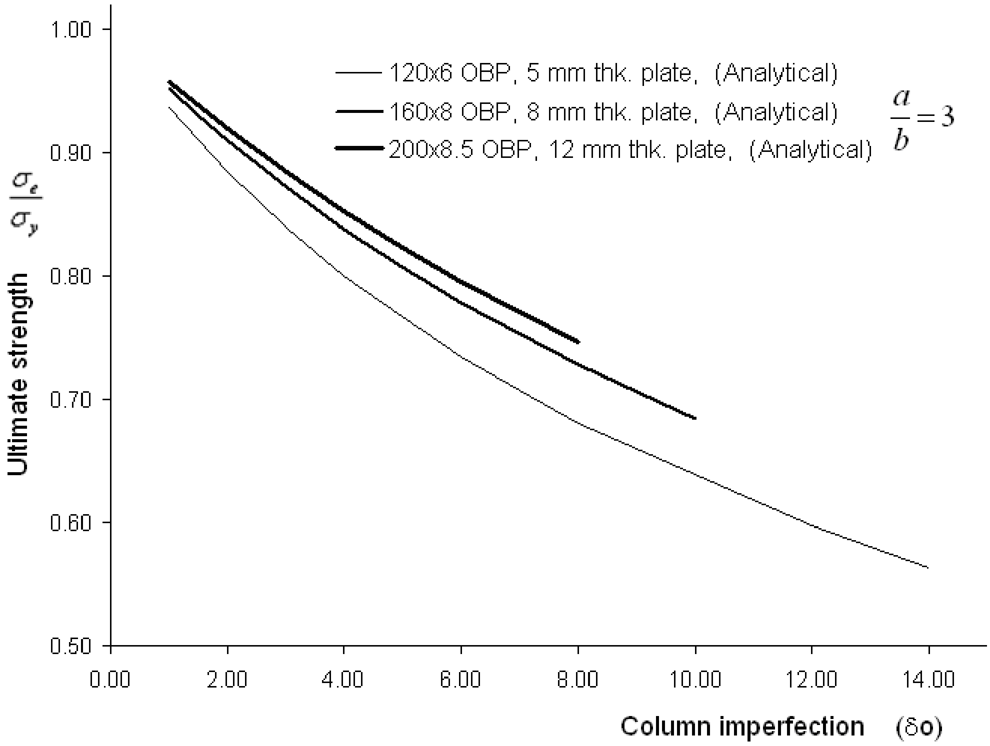

Figure 4. Effect of initial distortion on the Buckling strength of column according to Perry's formula

4. Finite Element Analysis

A 2D beam element (B21) is used for the column buckling and for the buckling strength evaluation of the equivalent columns. Four nodded reduced integration shell element (S4R) is used through out the structure as a homogeneous section uniformly for plate analysis. The material property is taken as of Lloyds' DH 36 grade steel. A bilinear material law has been applied without considering material non linearity. A static Riks load step is introduced to apply unit stress axially at one end. The opposite end kept fixed against axial movement to simulate the compression effect. The axial load is applied as small increments till it meets a stopping criterion either as a displacement or a load proportionality factor. The peak value of load from the load shortening curve is taken as the buckling strength of the stiffened plate in the post buckled condition.

4.1 Equivalent columns

The FE analysis is carried out for the same set of equivalent column models as shown in Figure 4 to validate the analytical relation. The section parameters of plate-stiffener combination are calculated based on the effective width of the plate. Pinned boundary conditions are used in this case to investigate the column behaviour.

The FE models are first used to find out the Euler critical buckling load and are verified analytically. These FE models are further used for the buckling strength analysis. The Figure 5 shows the comparison of analytical and FE results. It shows that the elastic limit approach is pessimistic and does not allow for post buckling elastic strength. Further, it appears that the analytical formula is incapable of accounting the strengthening capability of the asymmetrical cross-section with stiffener. A detailed investigation is required further to clarify and account for this post buckling elastic strength.

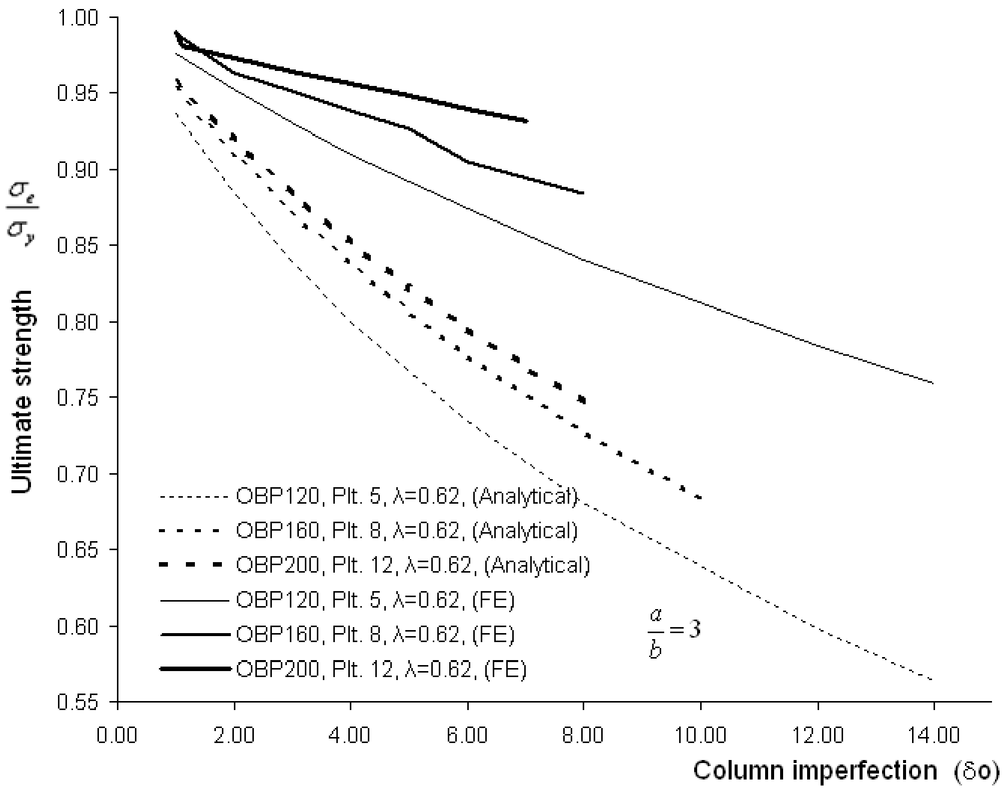

Figure 5. FE Buckling Analysis of an equivalent column

4.2 New strength parameter

It is quite common to use the non-dimensional ultimate strength, σ_u / σ_y to represent the strength of a structure in most of the ultimate strength studies carried out. But the post ultimate strength behaviour of the structure is important in the limit state design. Consider a ship structure with two upper decks ‘A’ and ‘B’ above the neutral axis with similar structural configuration. Deck ‘B’ is at mid way between the neutral axis and the highest deck ‘A’ as shown in Figure 6. During sagging (upper structure in compression), when the deck ‘A’ reaches ultimate strength, the lower deck ‘B’ still remains in the elastic region only half way towards the ultimate strength. When the load is further increased, if the highest deck ‘A’ exhibits poor post ultimate strength, the reserve strength from the mid deck ‘B’ is not achieved.

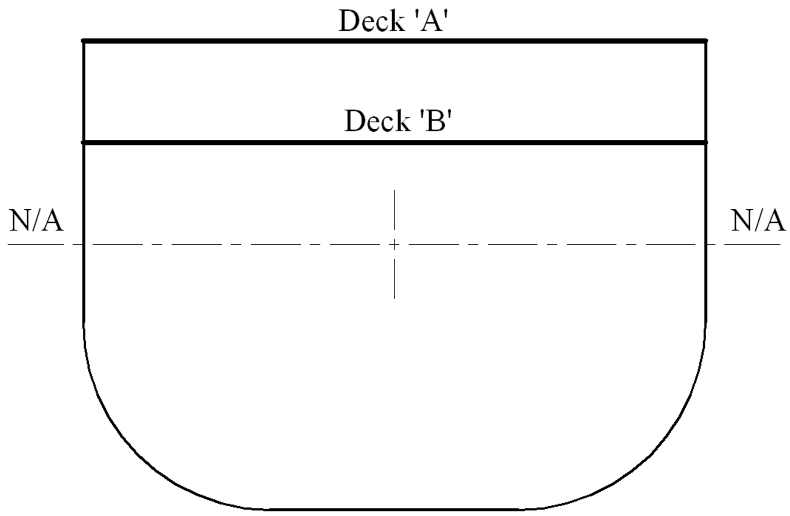

Figure 6. Upper decks ‘A’ and ‘B’

Thus deck ‘A’ should be designed with a characteristic similar to curve ‘B’. So when the structural strength of ship deck is being considered, a structure whose load shortening curve is relatively steady after the ultimate strength is preferred to the one with a higher ultimate strength value with a rapid fall in the curve exhibiting degraded behaviour. Since, both the decks ‘A’ and ‘B’ have similar structural configuration, the average of ultimate strength and the strength at double the ultimate strain provides a useful single measure of strength taking into account post ultimate behaviour.

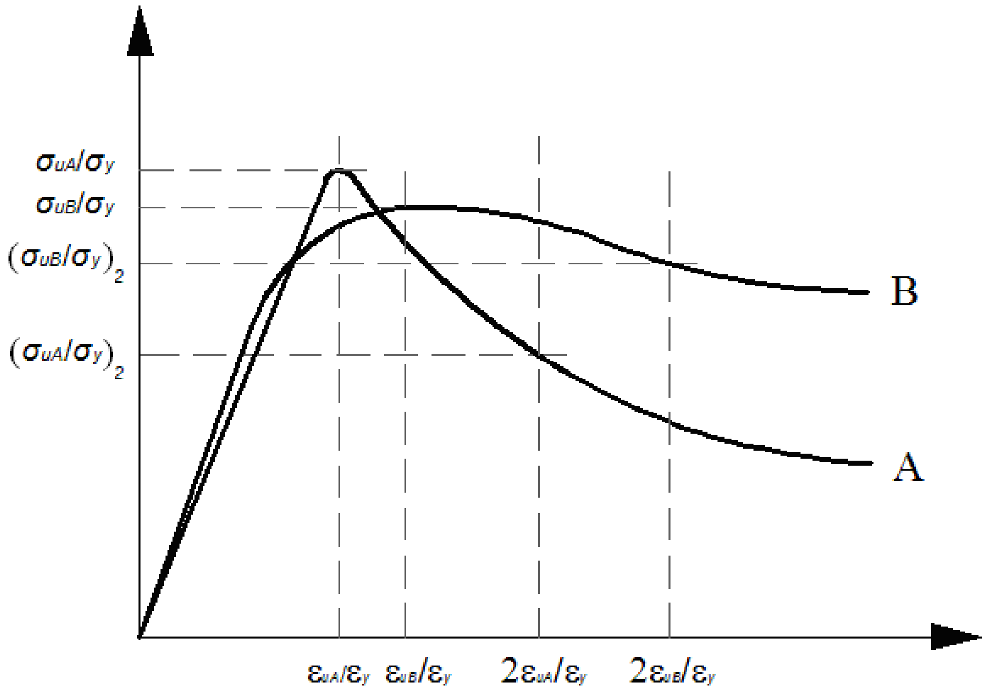

Figure 7. Post ultimate strength behaviour.

The Figure 7 shows the above discussed post ultimate behaviour for structural configurations ‘A’ and ‘B’. Hence it is proposed to take the strength parameter as,

$$S = \frac{\sigma_{u1} + \sigma_{u2}}{2\sigma_y} \qquad (4.1)$$

To obtain this parameter, the FE analysis should progress till the displacement value reaches two times the value corresponding to the peak load. The displacement should be adjusted accordingly to get this result for each case. The results of the analysis performed in this study are presented based on this new strength parameter.

4.3 Analysis of stiffened plates

Analysis is continued for a full bay model including four plate elements and three stiffeners as shown in Figure 8 and 9. Most of the tests were performed on panels with plate element aspect ratio of 1:3, and sinusoidal distortion. The sinusoidal initial distortion of the plate is assumed to be in sympathy with the aspect ratio of the plate elements. i.e. three waves longitudinally and one wave transversely. Adjacent transverse panels have opposite deflection. A smaller set of tests were carried out for models with unit aspect ratio plate elements and another set of models with the cusp shaped initial distortions. The distortion levels are sensitive to the aspect ratio of the plate as per the observation from a visit to the BVT construction site (Table 2 and Table 3) and this is substantiated by the values proposed by Smith (Smith et al. 1988).

To calibrate the FE procedure, the results obtained from FE analysis is compared with a proved analytical method proposed by (Pu, Das and Faulkner 1997). The method takes into account the initial distortion and the residual stress effects at a moderate level. Models as shown in Figure 8 with slight level of initial distortion without considering any residual stress effects were used for FE analysis. Table 4 shows the comparison and the deviation. Considering the above facts and the likely deviation while using finite element methods, the variation is found to be acceptable. This provides a ground to proceed with further trials required for the course of study.

Table 4. Comparison of FE and Analytical results

OBP	Plate thickness	Ultimate strength (σ_u/σ_y)		% Variation
		FE	Analytical	
OBP120x6	5mm	0.497	0.42	16.37
OBP160x8	8mm	0.608	0.56	7.97
OBP200x8.5	12mm	0.732	0.70	4.37

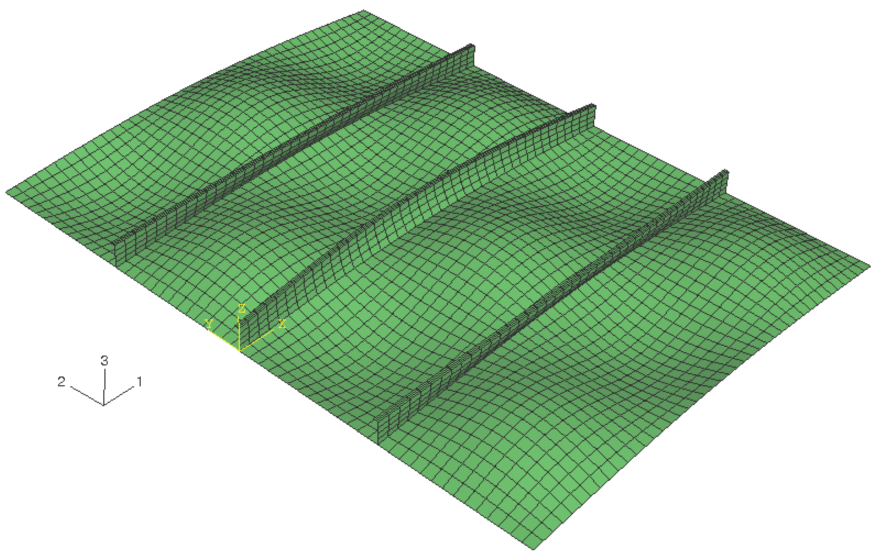

Figure 8. Sinusoidal form of distortion (Amplified), a/b=3

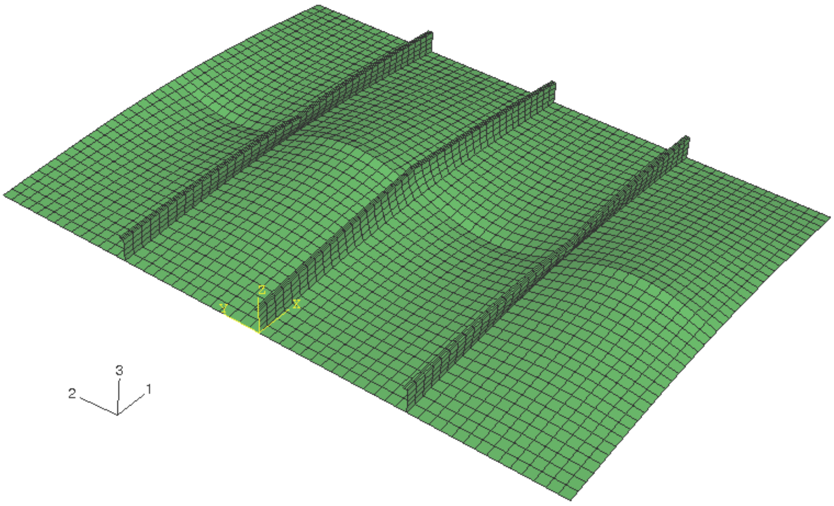

Figure 9. Cusp shaped distortion (Amplified), a/b=3

Figure 8 and 9 show the shape of initial distortion of the plate with sinusoidal and cusp shaped buckling modes respectively. Figure 10 and Figure 11 show the plots with corresponding failure mode and von mises stress.

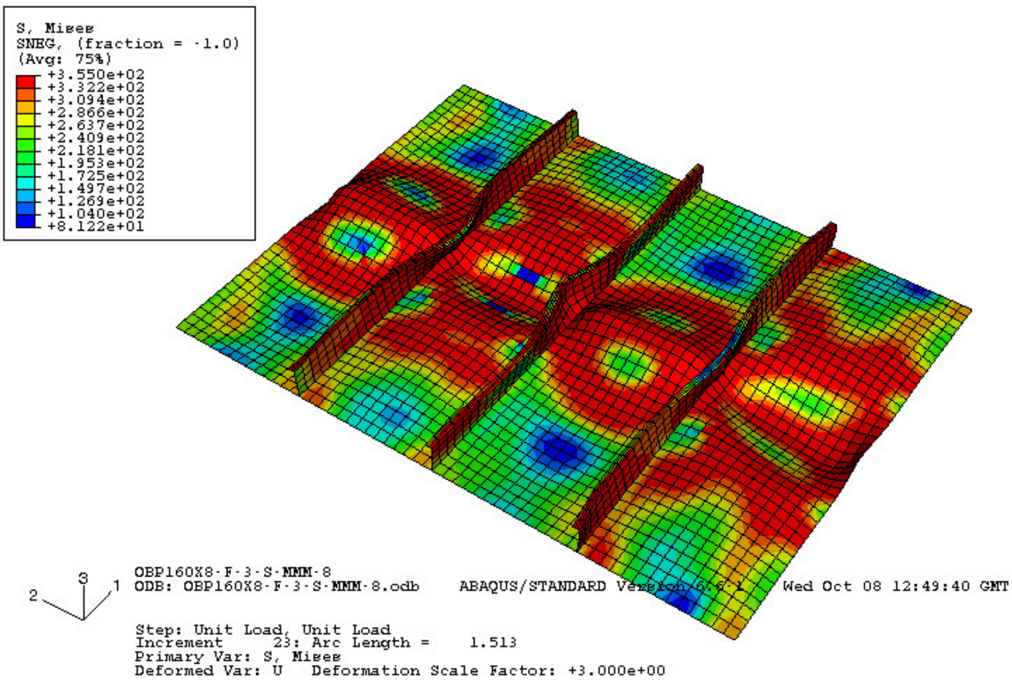

Figure 10. Buckled shape with sinusoidal distortion

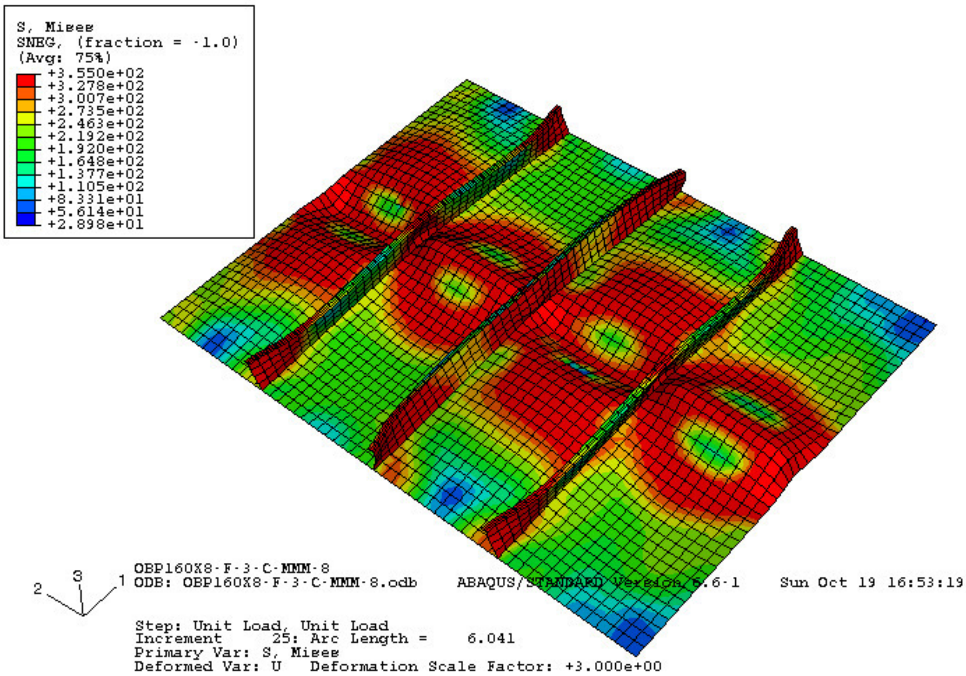

Figure 11. Buckled shape with cusp shaped distortion

5. Results and discussions

According to Golubitsky and Schaeffer (Thompson and Hunt, 1984), the imperfection sensitivity is closely related to the topological structural instability in certain bifurcation forms. When the axial compression is considered for structures, the line of resultant force will always be through the geometric centroid of the cross-section as the axial force is applied equally to the plate and stiffeners. The panel will always fail preferentially in the direction that puts the stiffener flange in compression. If the initial bowing distortion is positive (see Figure 1), opposing this effect, the panel will then tend to be inherently stronger.

5.1 Effect of Plate distortion

When the plate distortion increases from slight to severe amplitude and the stiffeners are relatively small, thick plates loose their strength in a more pronounced way. The thin plates preserve their strength or even show some increase in the strength in the respective distortion range. It is clear from Figure 12 that this trend varies uniformly as the plate thickness decreases. So the combined effect of geometrical properties of the section and the distortion are influencing the trend of strength variation.

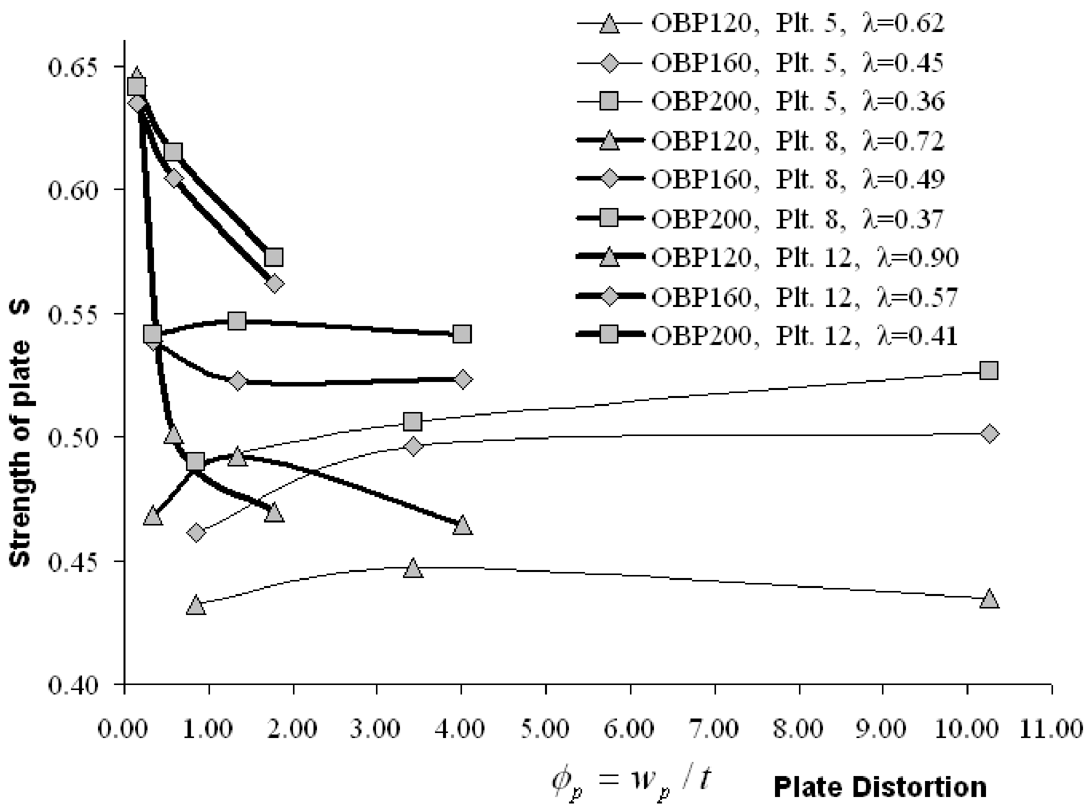

Figure 12. Strength against Sinusoidal Plate distortion (No bowing and warping), a/b=3.

The collapse of strength of the highest slenderness (stocky) panels (Figure 12) with the increase of initial distortion is evident when the plate thickness is mismatched with the stiffener size.

The results obtained are also plotted in Figure 13 in a manner similar to the Johnson parabola to represent the effect of distortion in combination with varying slenderness of the structure. The strength curves are plotted as iso-ϕ_p (plate distortion) lines. These plots point to the fact that axi-symmetrical structures would provide greater structural efficiency, e.g. a sandwich panel.

The studied structural configurations show a trend of the strength curves approaching the Johnson parabola as slenderness increases and as plate thickness increases. Figure 13 also indicates that the strength values of thin plated and medium plated structures are less affected by distortion.

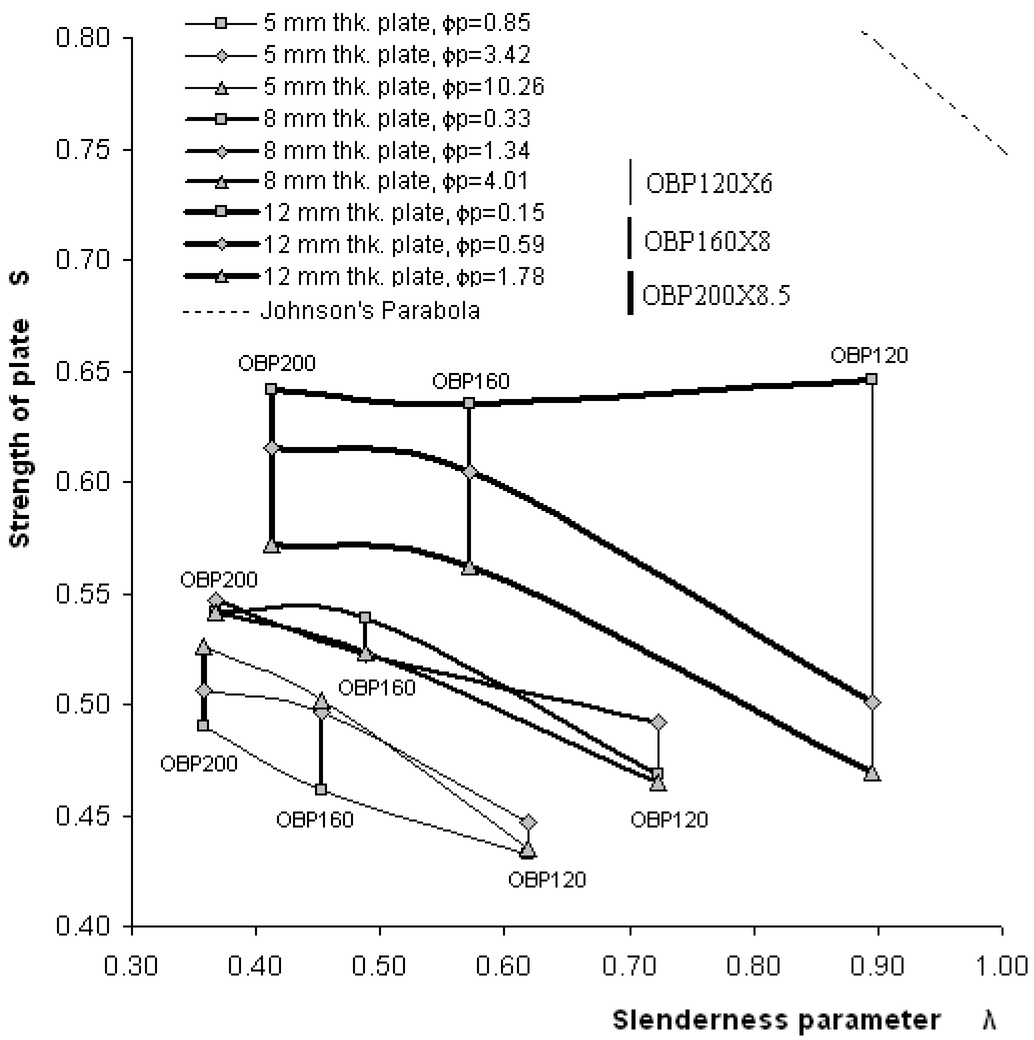

Figure 13. iso-ϕ_p lines with Sinusoidal distortion for a/b=3 (No bowing and warping).

5.2 Effect of Stiffener Bowing

All cases of stiffener bowing studied are in positive direction (see Figure 1). As the bowing of the stiffener increases, the strength was not found to vary appreciably as shown in Figure 14, apart from a heavily mismatched 12mm plate with OBP120x6 stiffener. This is similar to the effects seen with plate distortion. This is unexpected as it is usually assumed that a bowing type distortion should have significant effects on strength.

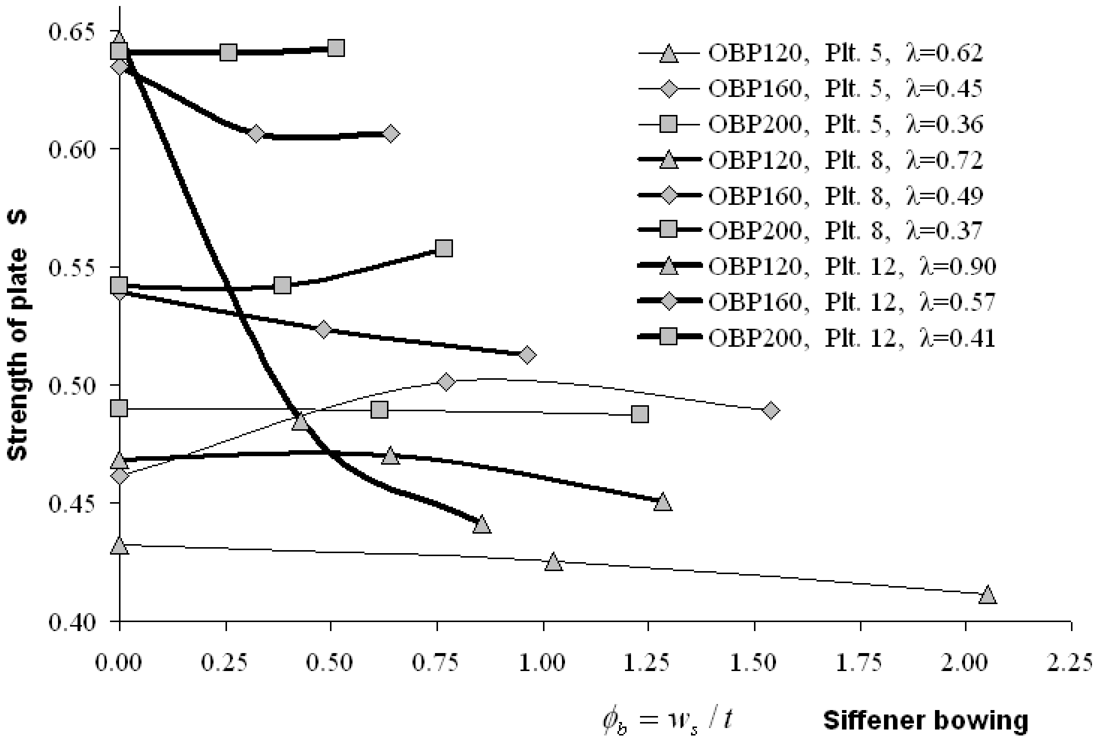

Figure 14. Strength against Sinusoidal Stiffener Bowing (Light plate distortion and no warping), a/b=3.

5.3 Effect of Stiffener Warping

Just like the case of bowing, warping in the selected range also is not producing much variation in the strength of the panels as shown in Figure 15. As the asymmetry of the OBP not really leads to failure in warping to one side, the plate failure then modifies this causing the stiffener to warp in sympathy, even if it is against the natural direction of failure (Figure 10). The only case that demonstrates significant variation is again the thick plate small stiffener case. However in this case a recovery of strength is apparent as the warping distortion increases. This can only be interpreted as a stiffening effect of the warped stiffener.

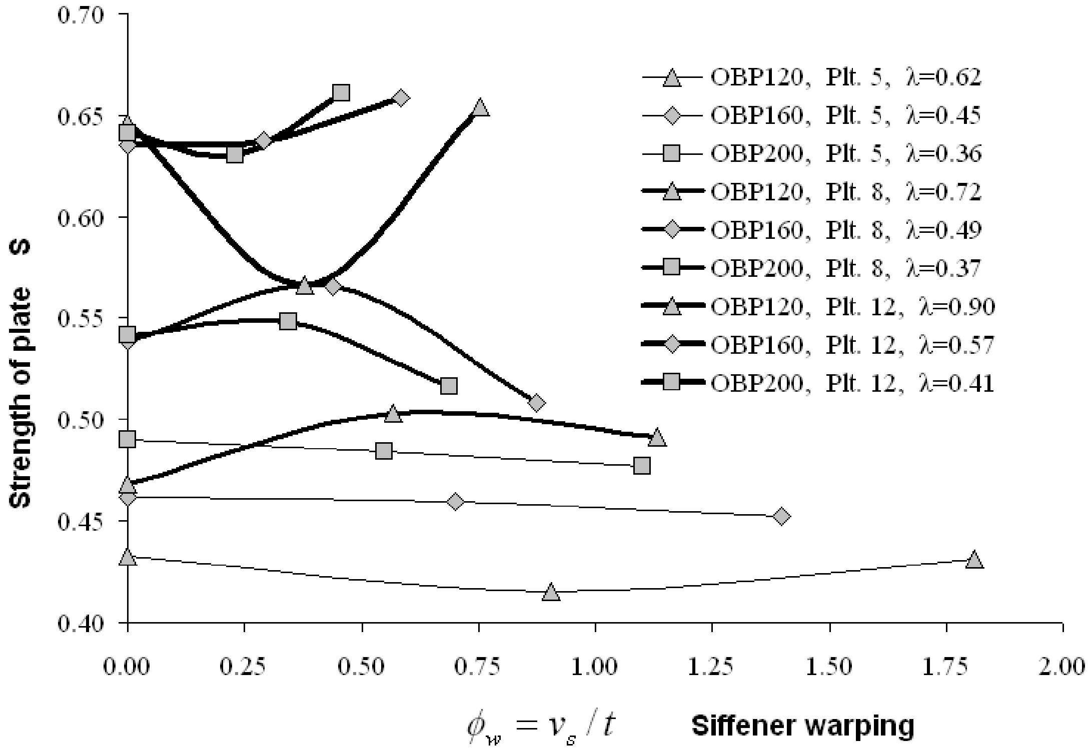

Figure 15. Strength against Sinusoidal Stiffener Warping (Light plate distortion and no bowing), a/b=3.

5.4 Effect of Cusp-shaped Plate Distortion

The strength of cusp shape follows similar trend as that of the sinusoidal distortion. When comparing with the sinusoidal type of distortion, the cusp shaped plates shows increased strength for thick plates and a decrease in strength for thinner plates for same amplitude of distortion as shown in Figure 16. It shows slight increase in the strength for some cases. This again clarifies that distorted geometry will not always reduce the strength of the stiffened plate.

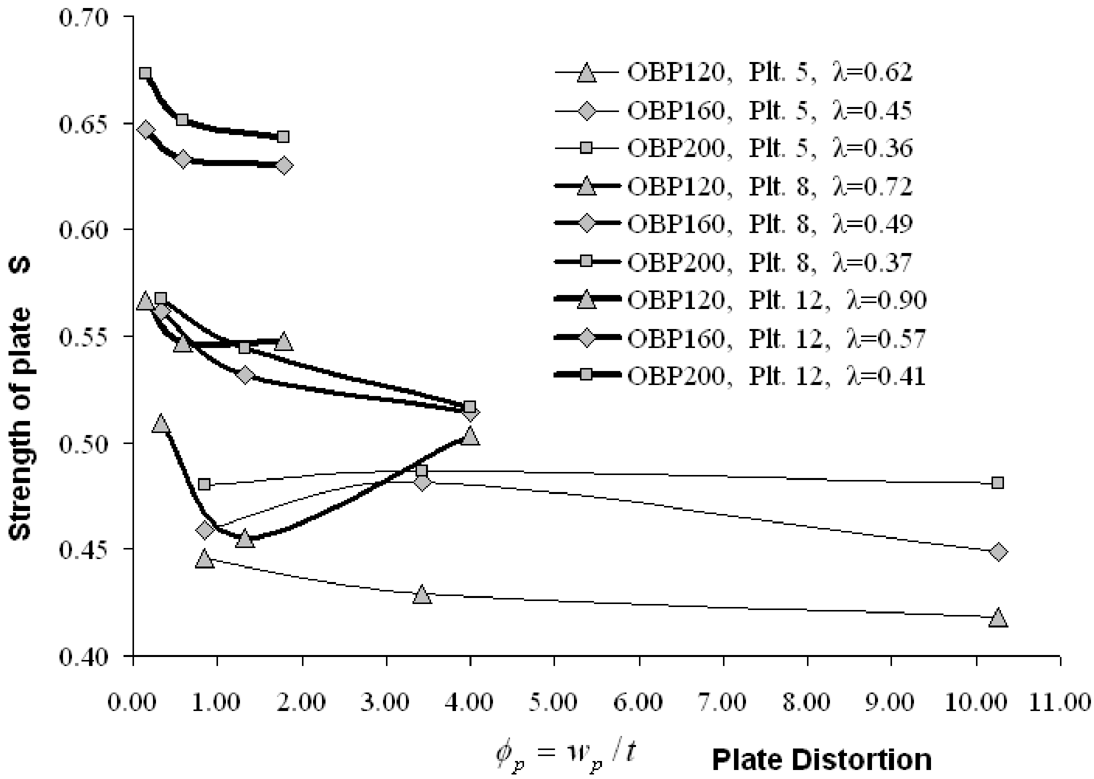

Figure 16. Strength against Cusp shaped Plate distortion (no bowing, no warping), a/b=3.

The cusp initial distortion with the single cycle over the length shows similar results for ultimate strength compared to the three cycle sinusoidal plate. Little variation is evident even for the thick plate small stiffener case. This indicates that the cusp type distortion provides a stiffening effect that tends to offset the effect of distortion itself. When the iso-ϕ_p lines are plotted for the cusp shaped distortion in Figure 17, even the thick plates show less variation of strength than for the sinusoidal case.

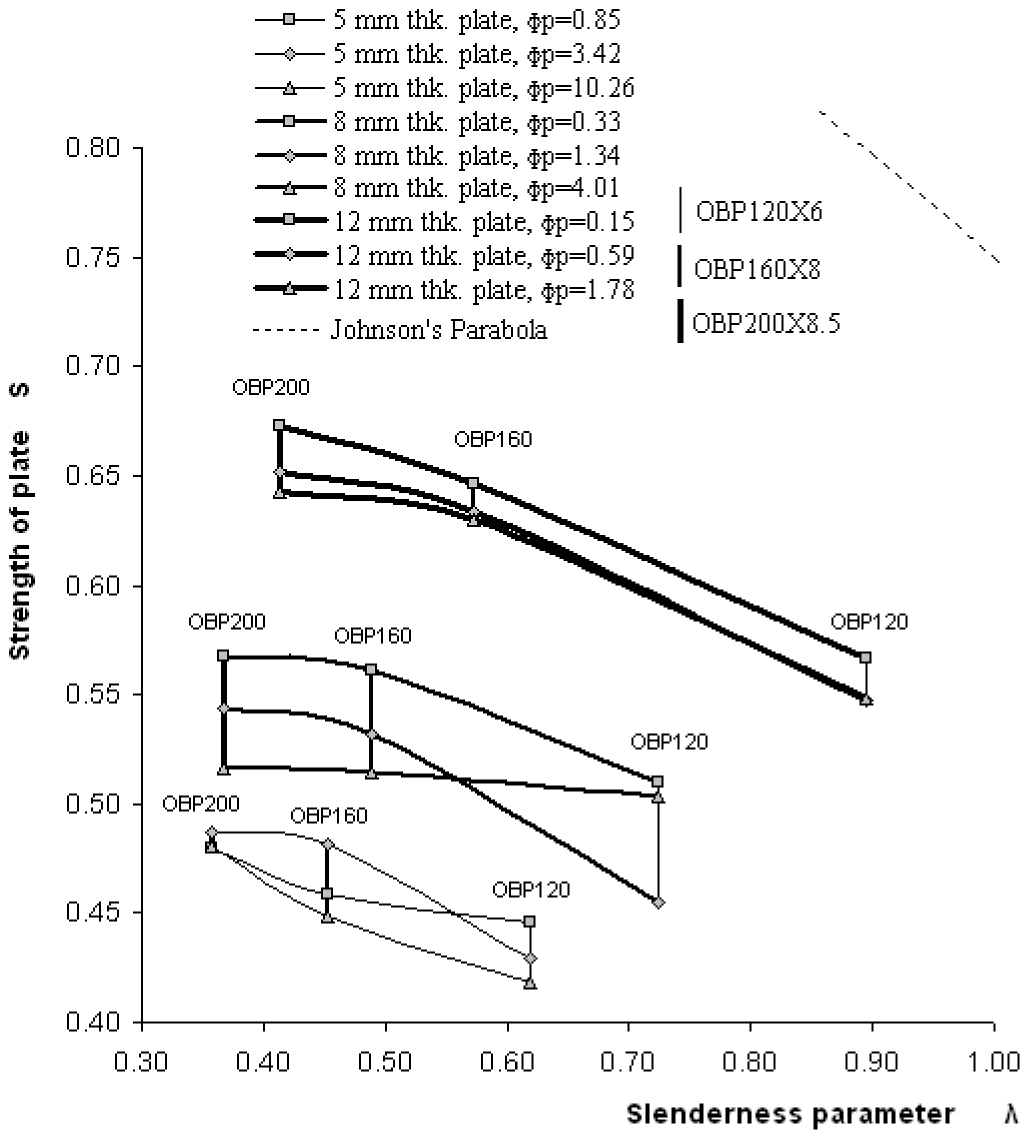

Figure 17. iso-ϕ_p lines with Cusp shaped distortion for a/b=3 (No bowing and warping).

5.5 Effect of Aspect ratio

When the aspect ratio of the plate element is reduced to 1 from 3, the strength of the plate-stiffener combinations is increased as expected. For the thin plates, as the distance between the plate and the neutral axis is greater, the distortion appears to increase the strength of the plate as shown in Figure 18.

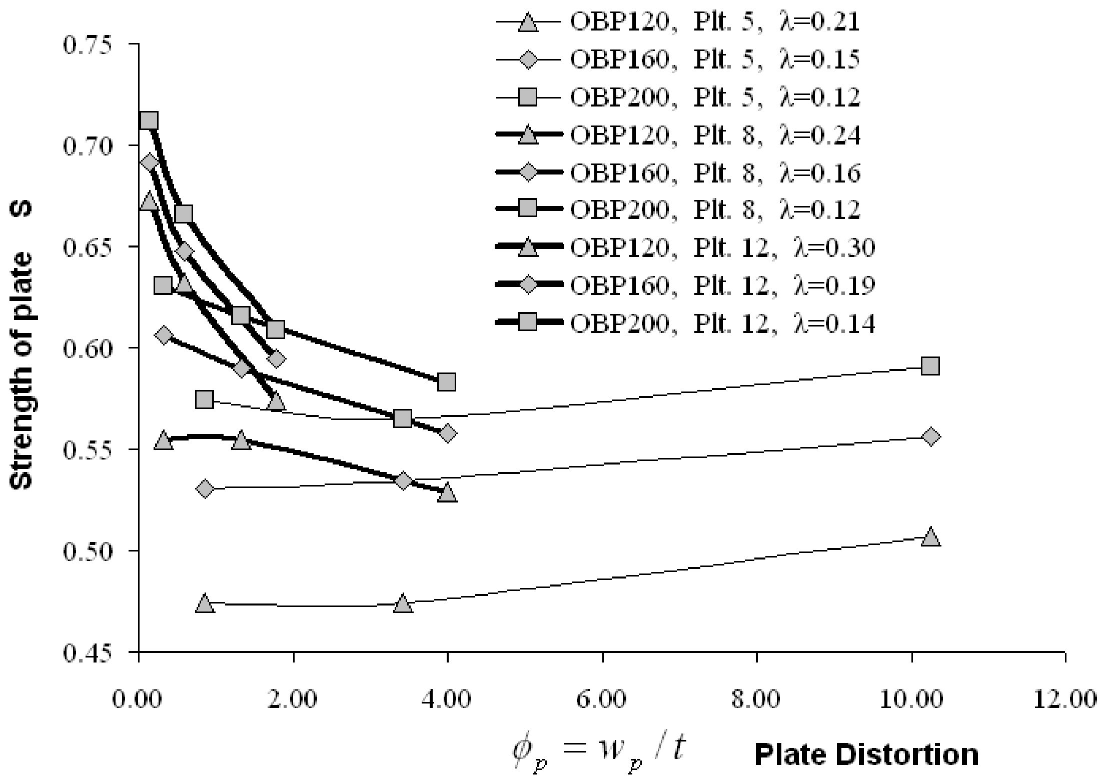

Figure 18. Strength against Plate distortion (no bowing, no warping) for a/b=1.

6. Conclusions

The conclusions from this study are as follows,

The equivalent column model using Perry's formula for first yield criteria shows clearly the effect of distortion and slenderness on the strength of the equivalent column. The FE analysis for the equivalent models shows that the post buckling behaviour has a significant effect, increasing strength over the predicted elastic case. So it appears to conclude that the initial distortion affects the strength of the stiffened plated structures. The further FE analysis of the panels modifies this conclusion.

For the relatively stocky panels chosen for this study and for the levels of distortions investigated, the ultimate strength of the panels does not seem to degrade as much as would be expected from single column type analysis.

The only combination of plate and stiffener that shows significant degradation of strength is the 12mm plate with OBP120x6 stiffener. This is recognised to be a mismatched combination and should be avoided in the design of such structures

Some combinations of plate distortion, stiffener bowing and stiffener warping appear to produce an increase of ultimate strength. This is an effect that requires further investigations.

A comparison of ultimate strength of 'cusp' type plate distortion as seen at plate butts in the shipyard, with a more conventional sinusoidal type of distortion seems to indicate that the 'cusp' type distortion is not significantly worse than the sinusoidal type.

This study has only considered geometrical initial distortion. Further studies are being undertaken to investigate the effects of residual stress as an additional influence on ultimate strength.

Additional benefits for ultimate strength are expected for axi-symmetric panels, e.g. sandwich panels and there is potential to investigate their use in ship structures.

Acknowledgement

The authors like to acknowledge BVT Surface Fleet Ltd. for providing the support for this work and the technical data.

References

Abaqus Version 6.6. Documentation collection.

Allen HG, Bulson PS. May 1980. Background to buckling. US: Mc graw-hill.

Dow RS, Smith CS. 1984. Effects of localized imperfections on compressive strength of long rectangular plates. Journal of Constructional Steel Research. 4: 51-76.

Faulkner D. 1975. A Review of Effective Steel Plating for Use in the Analysis of Stiffened Plating. Journal of Ship Research. 19: 1-17.

Hughes OF. 1988. Ship Structural Design: a rationally based, computer-aided optimization approach. New Jersey (US): The Society of Naval Architect and Marine Engineers.

Ozguc O, Das PK, Barltrop NDP. 2007. The new simple design equations for the ultimate compressive strength of imperfect stiffened plates. Ocean Engineering. 34(7): 970-986

Paik JK, Thayamballi AK. 2004. Ultimate Limit State Design of Steel-Plated Structures. West Sussex (England): John Wiley & Sons Ltd.

Pu Y, Das PK, Faulkner D. 1997. Ultimate compression strength and probabilistic analysis of stiffened Plates. Journal of OMAE. 119: 270–275.

Smith CS, Davidson PC, Chapman JC, Dowling PJ. 1988. Strength and stiffness of ships' plating under compression and tension. Transactions RINA. 130.

Thompson JMT, Hunt GW. 1984. Elastic instability phenomena. John Willy and Sons Ltd.

Troitsky MS. 1976. Stiffened Plates: Bending, Stability, and Vibrations. Elsevier Scientific Pub. Co.